

Regioselectivity of the ring-opening polymerization of monofunctional alkyl-substituted aromatic amine-based benzoxazines

H. Ishida*, D.P. Sanders

Department of Macromolecular Science and Engineering, Case Western Reserve University, Cleveland, OH 44106-7202, USA

Received 27 October 1999; received in revised form 26 May 2000; accepted 12 June 2000

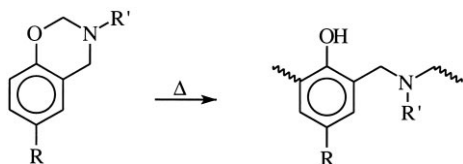
Abstract

The reaction site of the ring-opening polymerization in monofunctional aromatic amine-based benzoxazines has been investigated through systematic manipulation of the monomer chemistry. Selective protection or activation of sites on the arylamine ring towards electrophilic aromatic substitution has allowed a series of materials to be developed, which contain varying amounts of phenolic Mannich base bridges, arylamine Mannich base bridges, and methylene bridges. Electron-donating alkyl substituent groups at one or both meta positions on the arylamine ring facilitate ring opening/degradation at lower temperatures. This opening of rings in a step other than the polymerization reaction greatly increases the numbers of methylene linkages. Confirmation of the reaction sites was obtained via ^1H and ^{13}C NMR spectroscopy of oligomeric species. © 2001 Elsevier Science Ltd. All rights reserved.

Keywords: Polybenzoxazine; Benzoxazine; Thermosetting resin; Regioselectivity; Polymerization

1. Introduction

3-Substituted-3,4-dihydro-2H-1,3-benzoxazines have been shown to polymerize via a thermally induced ring-opening reaction to form a phenolic structure characterized by a Mannich base bridge ($-\text{CH}_2-\text{NR}-\text{CH}_2-$) as shown instead of the methylene bridge structure associated with traditional phenolic resins [1–4].



It has been demonstrated that the preferred reaction site is the position *ortho* to the hydroxyl functionality on the aromatic ring [2–6], although the *meta* positions of the aromatic ring can react at higher temperatures and/or very long cure times [5,7]. In the case of polybenzoxazines based on Bisphenol-A and aniline, analysis of the evolved gases from the thermally degrading resin showed the evolution of a *para*-methyl substituted aniline in addition to aniline [8]. To explain the presence of this evolved *p*-toluidine, it has been suggested that the pendant aromatic rings serve as additional sites for polymerization. This proposed mechanism

is in agreement with the solid-state ^{13}C and ^{15}N nuclear magnetic resonance (NMR) spectroscopic results by Russell et al. [5,6], although they have postulated that the predominant site of this side reaction is *ortho* to the amine substituent rather than *para* [8].

1,3,5-Triphenylhexahydro-1,3,5-triazine has also been shown to be an active intermediate and precursor in the synthesis of aromatic amine-based benzoxazine structures [9–12]. However, since no comprehensive NMR investigations of the curing of either phenolics with 1,3,5-triphenylhexahydro-1,3,5-triazine or the curing of neat 3-phenyl-3,4-dihydro-2H-1,3-benzoxazine has been reported, it has been difficult to determine the network structure of a number of polybenzoxazine thermosetting materials currently being investigated in our laboratory [12,13]. It would be advantageous to determine the relative numbers of arylamine rings that have reacted in these materials in order to make reasonable structure–property correlations.

A large volume of work has been done to determine the regioselectivity of the C-Mannich reaction as applied to phenolic substrates and has been reviewed by Tramontini et al. [13,14]. When the C-aminoalkylation reaction occurs on phenolic substrates, the predominant site of reaction is *ortho* to the phenolic moiety.

A few groups of researchers have been concerned with the regioselectivity of the Mannich reaction with respect to aromatic amines. Miocque and Vierfond [15–17] systematically studied the regioselectivity of a variety of

* Corresponding author. Tel: +1-216-368-4172; fax: +1-216-368-4202.
E-mail address: hxi3@po.cwru.edu (H. Ishida).

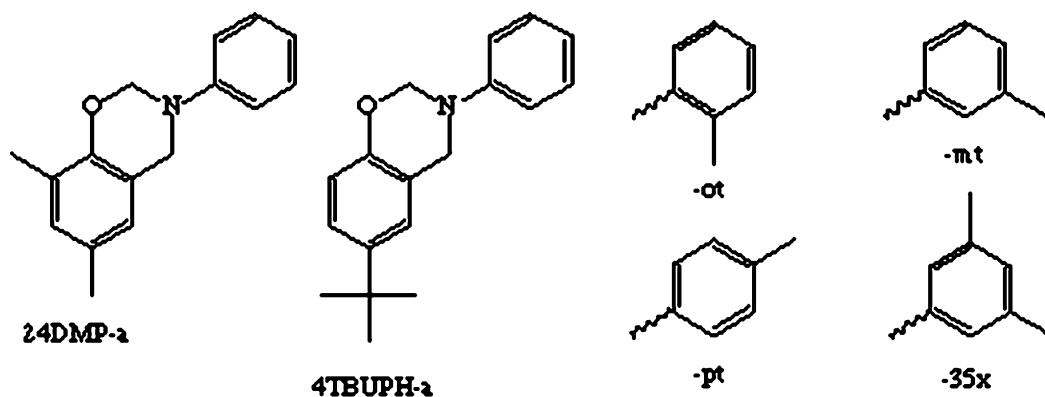


Fig. 1. Nomenclature of benzoxazine compounds.

arylamines when reacted with formaldehyde and various secondary aliphatic amines. In the reaction with *N,N*-dimethyl aniline, the Mannich reaction took place at the *para* position [15]. However, when there is a labile hydrogen on the nitrogen, aminoalkylation can take place at either the open *para* ring position or the nitrogen [16]. Under weakly acidic conditions, reaction at the nitrogen is preferred while under more strongly acidic conditions, the reaction at the *para*-position dominates. This is due to the fact that the carbon–nitrogen bond of the Mannich bridge cleaves under acidic conditions leaving only the more stable species, which have reacted at the *para* ring position [16]. Tsuchida et al. also examined the regioselectivity of *N*-methyl aniline [18–21]. Using the Mannich reaction with *N*-methyl aniline and either difunctional or primary amines, Tsuchida et al. were able to form oligomeric and low molecular weight polyamines. Under slightly different reaction conditions, the *N*-methyl aniline undergoes both *N*- and *C*-aminoalkylation reactions simultaneously.

Using various secondary and tertiary toluidines, Miocque and Vierfond examined the effect of adding a weakly activating methyl group on the regioselectivity of the Mannich reaction [17]. In the case of *N,N*-dimethyl-*o*-toluidine and *N,N*-dimethyl-*m*-toluidine, the reaction took place at the open *para* position. In the case of *N,N*-dimethyl-*p*-toluidine, no product was formed as the *ortho* position is too sterically hindered to react. When the additional methyl substituent was present to activate the ring towards electrophilic aromatic substitution, the aminoalkylation at the ring position took place under much less acidic conditions.

Unfortunately, no comprehensive analysis of the regioselectivity of the Mannich reaction has been undertaken when various phenolic and arylamine ring sites are simultaneously available. This paper will examine the regioselectivity of the benzoxazine polymerization using monofunctional benzoxazine monomers based on a variety of aromatic amines. Thermal polymerization of monofunctional benzoxazines typically does not yield high molecular weight linear polymers due to the competing depolymerization mechanisms [4]. The oligomeric products expected

from such a reaction will be soluble and, thereby, facilitate quantification of the reaction sites by NMR spectroscopy.

2. Experimental details

2.1. Materials

Monofunctional benzoxazine monomers were synthesized from 4-*t*-butyl phenol (Aldrich Chemical Co., 98%) and 2,4-dimethyl phenol (Aldrich Chemical Co., 98%). A series of aromatic amines (aniline (99%), *o*-toluidine (99 + %), *m*-toluidine (99%), *p*-toluidine (99%), and 3,5-xylidine (98%)] were purchased from Aldrich Chemical Co. All compounds were used as received without further purification. The monofunctional benzoxazines were synthesized via a solventless method discussed in full detail elsewhere [22]. The crude reaction products were dissolved in diethyl ether and washed with 2 N NaOH solution and rinsed with deionized water. The ether solutions were dried over sodium sulfate and the solvent was removed under vacuum. The compounds were sequentially recrystallized from methanol twice and finally ethanol once. The residual ethanol was removed under vacuum at room temperature for 24 h. Structures and nomenclatures for the monofunctional benzoxazine monomers are shown in Fig. 1.

2.2. 6,8-Dimethyl-3-phenyl-(2-methyl)-3,4-dihydro-2H-1,3-benzoxazine (24DMP-*ot*)

White needle-like crystalline powder. $^1\text{H NMR}$ (CDCl_3 , 200 MHz): δ 2.17 ppm (Ar-*p*- CH_3), δ 2.22 ppm (Ar-*o*- CH_3), δ 2.37 ppm (N-Ar- CH_3), δ 4.37 ppm (Ar- CH_2 -N), δ 5.17 ppm ($-\text{O}-\text{CH}_2-\text{N}-$), δ 6.5–7.5 ppm (Ar-H). FTIR (KBr): ν 756 and 725 cm^{-1} (*ortho*-substituted benzene); ν 1035 cm^{-1} (C–O str. aromatic ether); ν 1227 cm^{-1} (Ar–O–C asym. str. aromatic C–O); ν 933 cm^{-1} (oxazine ring). Purity by GC/MS: 99.3%.

Anal. Calcd. for $\text{C}_{17}\text{H}_{19}\text{NO}$: C, 80.60%; H, 7.56%; N, 5.53%. Found: C, 80.72%; H, 7.62%; N, 5.68%.

2.3. 6,8-Dimethyl-3-phenyl-(3-methyl)-3,4-dihydro-2H-1,3-benzoxazine (24DMP-mt)

Light tan crystalline powder. ^1H NMR (CDCl_3 , 200 MHz): δ 2.14 ppm (Ar-*p*-CH₃), δ 2.21 ppm (Ar-*o*-CH₃), δ 2.30 ppm (N-Ar-CH₃), δ 4.56 ppm (Ar-CH₂-N), δ 5.33 ppm (-O-CH₂-N-), δ 6.5–7.5 ppm (Ar-H). FTIR (KBr): ν 778 and 695 cm^{-1} (*meta*-substituted benzene); ν 1033 cm^{-1} (C-O str. aromatic ether); ν 1222 cm^{-1} (Ar-O-C asym. str. aromatic C-O); ν 940 cm^{-1} (oxazine ring). Purity by GC/MS: 99.3%.

Anal. Calcd. for $\text{C}_{17}\text{H}_{19}\text{NO}$: C, 80.60%; H, 7.56%; N, 5.53%. Found: C, 80.39%; H, 7.53%; N, 5.78%.

2.4. 6,8-Dimethyl-3-phenyl-(4-methyl)-3,4-dihydro-2H-1,3-benzoxazine (24DMP-pt)

White plate-like crystalline powder. ^1H NMR (CDCl_3 , 200 MHz): δ 2.13 ppm (Ar-*p*-CH₃), δ 2.21 ppm (Ar-*o*-CH₃), δ 2.26 ppm (N-Ar-CH₃), δ 4.53 ppm (Ar-CH₂-N), δ 5.31 ppm (-O-CH₂-N-), δ 6.5–7.5 ppm (Ar-H). FTIR (KBr): ν 1515 and 820 cm^{-1} (*para*-substituted benzene); ν 1032 cm^{-1} (C-O str. aromatic ether); ν 1226 cm^{-1} (Ar-O-C asym. str. aromatic C-O); ν 944 cm^{-1} (oxazine ring). Purity by GC/MS: 99.8%.

Anal. Calcd. for $\text{C}_{17}\text{H}_{19}\text{NO}$: C, 80.60%; H, 7.56%; N, 5.53%. Found: C, 80.81%; H, 7.70%; N, 5.68%.

2.5. 6,8-Dimethyl-3-phenyl-(3,5-dimethyl)-3,4-dihydro-2H-1,3-benzoxazine (24DMP-35x)

White crystalline powder. ^1H NMR (CDCl_3 , 200 MHz): δ 2.14 ppm (Ar-*p*-CH₃), δ 2.21 ppm (Ar-*o*-CH₃), δ 2.26 ppm (N-Ar-CH₃), δ 4.55 ppm (Ar-CH₂-N), δ 5.32 ppm (-O-CH₂-N-), δ 6.5–7.5 ppm (Ar-H). FTIR (KBr): ν 833 and 695 cm^{-1} (1,3,5-trisubstituted benzene); ν 1037 cm^{-1} (C-O str. aromatic ether); ν 1223 cm^{-1} (Ar-O-C asym. str. aromatic C-O); ν 940 cm^{-1} (oxazine ring). Purity by GC/MS: 99.5%.

Anal. Calcd. for $\text{C}_{18}\text{H}_{21}\text{NO}$: C, 80.86%; H, 7.92%; N, 5.24%. Found: C, 81.09%; H, 7.97%; N, 5.14%.

2.6. 3-Phenyl-6-*t*-butyl-3,4-dihydro-2H-1,3-benzoxazine (4TBUPH-a)

White crystalline powder. ^1H NMR (CDCl_3 , 200 MHz): δ 1.27 ppm (*t*-bu-CH₃), δ 4.64 ppm (Ar-CH₂-N), δ 5.34 ppm (-O-CH₂-N-), δ 6.5–7.5 ppm (Ar-H). FTIR (KBr): ν 756 and 694 cm^{-1} (monosubstituted benzene); ν 1031 cm^{-1} (C-O str. aromatic ether); ν 1234 cm^{-1} (Ar-O-C asym. str. aromatic C-O); ν 951 cm^{-1} (oxazine ring). Purity by GC/MS: 99.3%.

Anal. Calcd. for $\text{C}_{18}\text{H}_{21}\text{NO}$: C, 80.86%; H, 7.92%; N, 5.24%. Found: C, 81.06%; H, 7.77%; N, 5.39%.

2.7. 3-Phenyl-(2-methyl)-6-*t*-butyl-3,4-dihydro-2H-1,3-benzoxazine (4TBUPH-ot)

White needle-like crystalline powder. ^1H NMR (CDCl_3 , 200 MHz): δ 1.27 ppm (*t*-bu-CH₃), δ 2.38 ppm (N-Ar-CH₃), δ 4.41 ppm (Ar-CH₂-N), δ 5.16 ppm (-O-CH₂-N-), δ 6.5–7.5 ppm (Ar-H). FTIR (KBr): ν 768 and 724 cm^{-1} (*ortho*-substituted benzene); ν 1033 cm^{-1} (C-O str. aromatic ether); ν 1235 cm^{-1} (Ar-O-C asym. str. aromatic C-O); ν 944 cm^{-1} (oxazine ring). Purity by GC/MS: 97.1%.

Anal. Calcd. for $\text{C}_{19}\text{H}_{23}\text{NO}$: C, 81.10%; H, 8.24%; N, 4.98%. Found: C, 81.22%; H, 8.22%; N, 5.02%.

2.8. 3-Phenyl-(3-methyl)-6-*t*-butyl-3,4-dihydro-2H-1,3-benzoxazine (4TBUPH-mt)

Light tan crystalline powder. ^1H NMR (CDCl_3 , 200 MHz): δ 1.27 ppm (*t*-bu-CH₃), δ 2.31 ppm (N-Ar-CH₃), δ 4.63 ppm (Ar-CH₂-N), δ 5.33 ppm (-O-CH₂-N-), δ 6.5–7.5 ppm (Ar-H). FTIR (KBr): ν 777 and 695 cm^{-1} (*meta*-substituted benzene); ν 1030 cm^{-1} (C-O str. aromatic ether); ν 1235 cm^{-1} (Ar-O-C asym. str. aromatic C-O); ν 950 cm^{-1} (oxazine ring). Purity by GC/MS: 99.6%.

Anal. Calcd. for $\text{C}_{19}\text{H}_{23}\text{NO}$: C, 81.10%; H, 8.24%; N, 4.98%. Found: C, 81.31%; H, 8.36%; N, 5.12%.

2.9. 3-Phenyl-(4-methyl)-6-*t*-butyl-3,4-dihydro-2H-1,3-benzoxazine (4TBUPH-pt)

White plate-like crystalline powder. ^1H NMR (CDCl_3 , 200 MHz): δ 1.27 ppm (*t*-bu-CH₃), δ 2.26 ppm (N-Ar-CH₃), δ 4.60 ppm (Ar-CH₂-N), δ 5.31 ppm (-O-CH₂-N-), δ 6.5–7.5 ppm (Ar-H). FTIR (KBr): ν 1515 and 818 cm^{-1} (*para*-substituted benzene); ν 1034 cm^{-1} (C-O str. aromatic ether); ν 1233 cm^{-1} (Ar-O-C asym. str. aromatic C-O); ν 948 cm^{-1} (oxazine ring). Purity by GC/MS: 99.7%.

Anal. Calcd. for $\text{C}_{19}\text{H}_{23}\text{NO}$: C, 81.10%; H, 8.24%; N, 4.98%. Found: C, 81.09%; H, 8.21%; N, 5.09%.

2.10. 3-Phenyl-(3,5-dimethyl)-6-*t*-butyl-3,4-dihydro-2H-1,3-benzoxazine (4TBUPH-35x)

Yellowish viscous liquid. ^1H NMR (CDCl_3 , 200 MHz): δ 1.27 ppm (*t*-CH₃), δ 2.27 ppm (N-Ar-CH₃), δ 4.61 ppm (Ar-CH₂-N), δ 5.31 ppm (-O-CH₂-N-), δ 6.5–7.5 ppm (Ar-H). FTIR (KBr): ν 833 and 695 cm^{-1} (1,3,5-trisubstituted benzene); ν 1030 cm^{-1} (C-O str. aromatic ether); ν 1232 cm^{-1} (Ar-O-C asym. str. aromatic C-O); ν 947 cm^{-1} (oxazine ring). Purity by GC/MS: 96.8%.

Anal. Calcd. for $\text{C}_{20}\text{H}_{25}\text{NO}$: C, 81.31%; H, 8.53%; N, 4.74%. Found: C, 81.57%; H, 8.33%; N, 4.80%.

2.11. Methods

The structure of the monomers was confirmed via proton

Table 1
Calorimetric properties of 2,4-dimethyl phenol-based benzoxazine monomers

	Melting temperature (°C)	Peak exotherm (°C)	Heat of reaction (J/g)
24DMP-ot	67.9	–	–
24DMP-mt	52.9	282.9	170.7
24DMP-pt	73.6	285.6	159.8
24DMP-35x	97.9	269.8	170.9

(^1H) and carbon (^{13}C) nuclear magnetic resonance (NMR) spectroscopy. The NMR was performed on a Varian 200 MHz Gemini NMR spectrometer. Deuterated chloroform was used as the solvent. The ^1H and ^{13}C NMR spectra of the monomers were obtained with 64 and 2000 transients, respectively. All peaks were referenced with respect to tetramethylsilane (TMS). The purity of the synthesized compounds was determined by gas chromatography/mass spectroscopy (GC/MS) and elemental analysis (M-H-W Laboratories, Phoenix, Az.). GC/MS was performed with a Hewlett–Packard 6890 Gas Chromatograph coupled with a 5973 Mass Selective Detector. Fourier transform infrared (FTIR) spectra of the monomers cast onto KBr plates from CHCl_3 solution were obtained on a Bomem Michelson MB-110 spectrometer with a KBr beamsplitter and liquid nitrogen-cooled mercury–cadmium–telluride (MCT) detector with dry purge gas supplied from a Whatman 75-62 FTIR Purge Gas Generator. The spectrometer was operated at a resolution of 4 cm^{-1} . The reaction exotherms of the monomers were measured using differential scanning calorimetry (DSC) with a TA Instruments DSC 2910 High Pressure Differential Scanning Calorimeter. Samples were run in hermetic aluminum sample pans with small holes in the upper lids. The DSC cell was

pressurized with nitrogen at 2.76 MPa while the temperature was ramped at $10^\circ\text{C}/\text{min}$.

The benzoxazines were reacted under an argon atmosphere in NMR tubes with and without phenolic initiators. The ^1H and ^{13}C NMR spectra of the polymerized compounds were obtained by recording 64 and 2000 transients, respectively. The molecular weight of the resulting polymers was determined via size exclusion chromatography (SEC) using a Waters 510 HPLC pump with a U6K injector and a Waters 484 Tunable Absorbance ($\lambda = 254\text{ nm}$) and Waters 410 Refractive Index detectors with tetrahydrofuran (THF) as the elution solvent. The columns were Whatman Styragel 50, 10^2 and 10^3 nm SEC columns.

Degraded network fragments were produced by thermogravimetric analysis (TGA) using a TA Instruments Hi-Res 2950 Thermogravimetric Analyzer equipped with a Evolved Gas Analysis (EGA) furnace. The temperature was ramped at $10^\circ\text{C}/\text{min}$ under a nitrogen atmosphere. Evolved gases from the thermally degraded materials were trapped by bubbling the evolved gas through HPLC grade chloroform. Mass identification was performed via GC/MS. The 50 largest chromatogram peaks in each sample were integrated. Compounds were identified using a NIST Mass Spectral Library, Nbs75 k. Final assignments were identified by injecting solutions of the pure compounds.

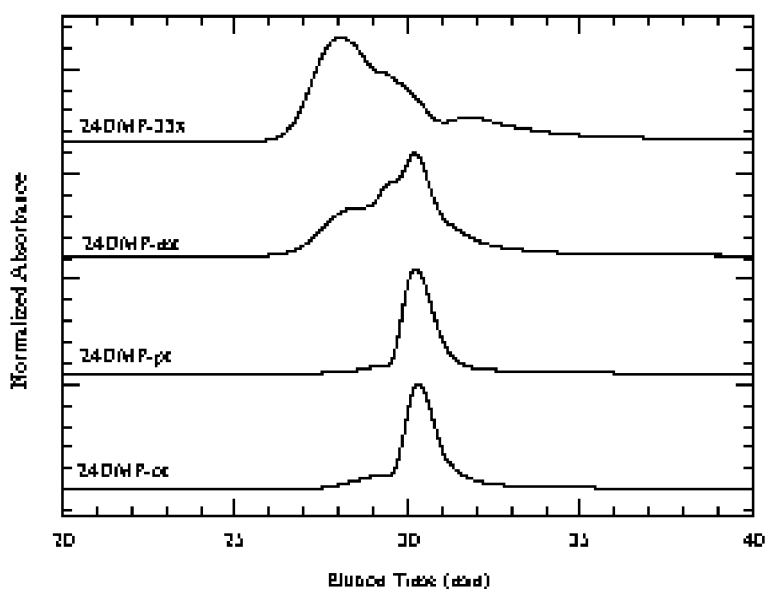


Fig. 2. SEC chromatograms of reacted 24DMP-based monomers.

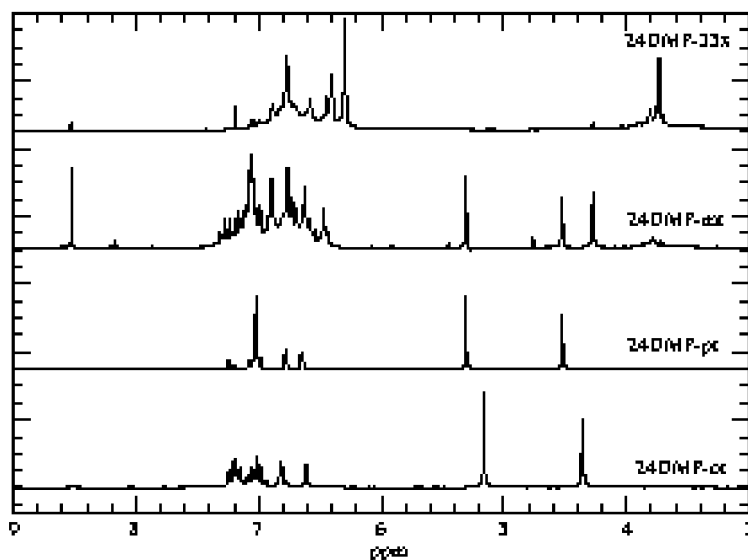


Fig. 3. ^1H NMR spectra of reacted 24DMP-based monomers.

3. Results and discussion

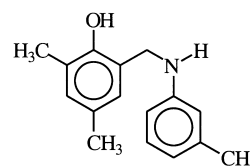
3.1. 2,4-Dimethyl phenol-based monomers

The calorimetric properties of the 24DMP-based benzoxazines are listed in Table 1. The peak temperature of the reaction exotherm decreases as the number of methyl substituents in the *meta* position on the arylamine ring increases. It is suspected that 24DMP-ot merely degrades at higher temperatures. The presence of a reaction exotherm in these materials is surprising since the primary site of reaction has been blocked. The low heats of reaction suggest that these exotherms may simply represent the ring-opening and/or cleaving. The slight difference among 24DMP-mt, 24DMP-35x, and 24DMP-pt may be due to either polymerization to activated sites on the arylamine ring or another side reaction.

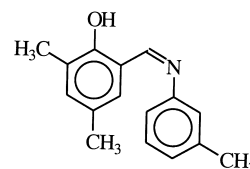
After reaction of the 24DMP-based compounds under argon for 3 h at 200°C, the molecular weight distribution of the polymerized species were examined via SEC as shown in Fig. 2. Each SEC chromatogram has been normalized to the height of the highest absorbance peak. The retention time of the monomeric species is about 30.2 min. 24DMP-ot and 24DMP-pt show the development of only a small shoulder at around 29.2 min, which is typical for an open-ring monomeric species. 24DMP-mt also shows this open ring species as well but additionally exhibits larger molecular weight species with a peak centered at 28.4 min. The higher molecular weight species are also present in the reacted 24DMP-35x. No attempt to determine the molecular weight distribution will be made except to comment that the higher molecular weight species are probably primarily dimeric in nature with smaller additional amounts of higher oligomers such as trimers and tetramers.

3.2. ^1H NMR spectroscopy

These results are corroborated by ^1H NMR spectroscopy as shown in Fig. 3. In 24DMP-ot and 24DMP-pt, the resonances corresponding to the oxazine ring methylene protons are clearly evident near 4.5 and 5.3 ppm [23]. Since no methylene peaks attributable to oligomeric or open ring species are easily observed, these two materials did not react during the exposure to higher temperature. However, 24DMP-mt shows a resonance at 4.27 ppm, which has been previously assigned to the open ring methylene protons of a Mannich base [23].



Another prominent resonance corresponding to a methine proton of a free aromatic Schiff base can be observed at 8.52 ppm.



The development of a number of resonances in the range of 3.6–3.9 ppm is also observed and will be discussed later.

In the case of 24DMP-35x, the resonances corresponding to the closed oxazine ring methylene protons have completely disappeared and only a small amount of Mannich base and Schiff base species are observed. Resonances in the region of 3.6–3.9 ppm become even more prevalent in the reacted 24DMP-35x material.

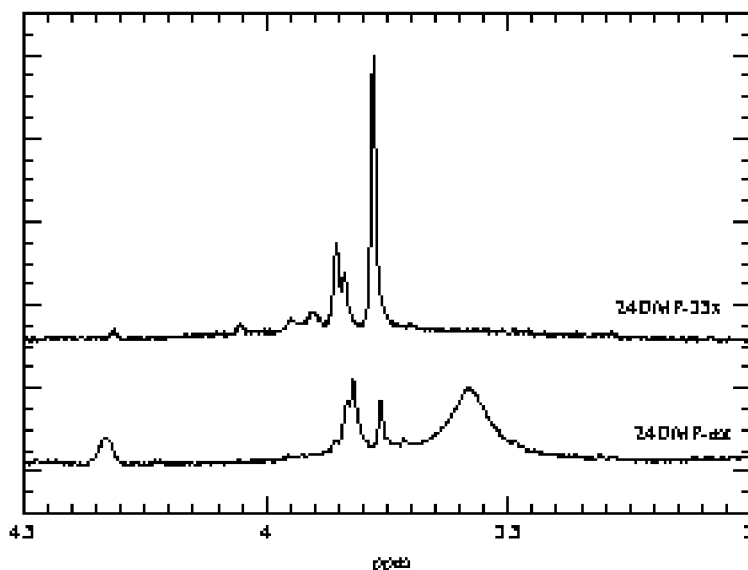
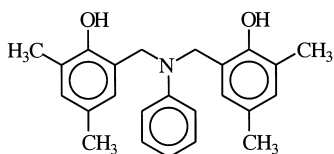


Fig. 4. Methylene region of ^1H NMR spectra of reacted 24DMP-mt and 24DMP-35x.

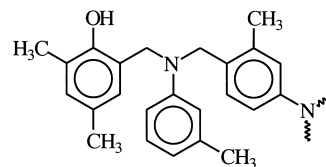
Blocking the preferred site of reaction, i.e. the site *ortho* to the phenolic position, with the methyl substituent was effective in preventing the ring-opening from occurring in 24DMP-ot and 24DMP-pt. Activating the arylamine ring with methyl substituents at one or both *meta* positions facilitated the formation of the open-ring species at lower temperatures. This is surprising since previous NMR studies on the hydrolytic stability of a similar series of monofunctional benzoxazines based upon aniline, *m*-toluidine, *o*-toluidine, and *p*-toluidine would suggest that the rings of 24DMP-ot should be most susceptible to opening [24] while those of 24DMP-pt should be the most stable. The presence of methyl substituents in the meta positions may allow for sufficient electron density to be pushed into the oxazine ring, without the formation of resonance structures, such that the oxazine rings are more reactive.

The methylene region of the ^1H NMR spectra of 24DMP-mt and 24DMP-35x cured under more optimal conditions (at 200°C for 2–3/4 h and at 190°C for 2 h/at 200°C for 1 h, respectively) are shown in Fig. 4. In 24DMP-mt, a broad resonance near 4.34 ppm is observed. Previous work has shown that the methylene protons of the model dimeric species based upon 2,4-dimethyl phenol and aniline absorb near 4.3 ppm [25].



This type of linkage will be referred to as a phenolic Mannich bridge. Therefore, the proton resonance at 4.34 ppm can be reasonably assigned to the methylene protons in the phenolic Mannich bridge structure. However,

since the *ortho* phenolic sites were specifically blocked with a methyl substituent in this 24DMP-mt, no available *ortho* phenolic sites are available to produce the model dimeric compound (*N,N*-bis(2-hydroxy-3,5-dimethyl benzene)aniline) mentioned previously, the reaction site is shifted to available sites on the arylamine ring as pictured.



This type of linkage will be referred to as an arylamine Mannich bridge. The environments of the methylene protons on the carbon connected to the phenolic ring and the methylene protons on the carbon connected to the arylamine ring are similar and thus the two resonances cannot be resolved. Additionally, a large broad resonance centered at 3.58 ppm is assigned to the protons on the free amine via comparison with reference spectra [26].

The resonance assigned to the arylamine Mannich bridge methylene protons is small in 24DMP-35x suggesting that few sites on the arylamine ring have served as sites for polymerization. However, the methylene resonances in the region of 3.7–3.9 ppm are greatly enhanced. Three predominant resonances can be seen centered at 3.86, 3.84, and 3.78 ppm.

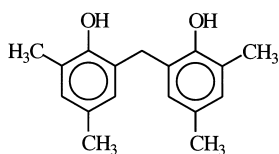
Solomon et al. [27–35] showed that methylene bridges can be formed as a result of cleavage of the Mannich bridge, and subsequent attack of the resulting quinone methide on another phenolic ring. In the model reactions based on 2,4-dimethyl phenol, the *ortho-ortho*

Table 2
Evolved gas analysis (GC/MS) of 24DMP-mt and 24DMP-35x reacted with 17 wt% *p*-cresol

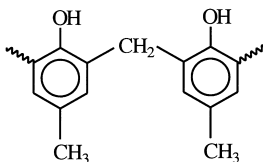
Retention time (min)	Evolved species	Parent ion (<i>m/z</i>)	Assigned ^a	24DMP-35x (%)	24DMP-mt (%)
2.54	Toluene	92	L,M,N	0.48	0.18
3.51	<i>p</i> -Xylene	106	L,M,N	0.06	
3.61	<i>m</i> -Xylene	106	L,M,N	0.34	0.32
3.94	Ethylbenzene	106	M,N	0.05	0.05
5.10	1,3,5-Trimethyl benzene	120	M,N	0.36	0.34
5.18	Phenol	94	L,M,N		0.15
5.54	1,2,4-Trimethylbenzene	120	M,N	0.17	0.10
6.52	<i>o</i> -Cresol	108	L,M,N	0.34	0.55
6.68	1-Ethyl-3,5-dimethyl benzene	134	N,P		0.02
6.87	<i>p</i> -Cresol	108	L,M,N	1.25	4.07
7.04	<i>m</i> -Toluidine	107	M,N	–	22.16
7.54	2,6-Dimethyl phenol	122	L,M,N	0.37	0.32
7.85	1,2,3,5-Tetramethylbenzene	134	N	0.06	0.04
8.25	2,4-Dimethyl phenol	122	M,N	23.48	21.82
8.62	<i>N</i> -Methyl- <i>m</i> -toluidine	121	M,N	0.07	0.62
8.76	2,5-Dimethyl aniline	121	M,N	–	0.63
8.82	3,5-Xylidine	121	M,N	16.62	
9.22	3,4-Dimethyl aniline	121	M,N	–	0.86
9.31	2,4,6-Trimethyl phenol	136	M,N	44.74	30.49
10.33	<i>N</i> -Methyl-3,5-xylidine	135	M,N	0.91	
11.03	3,4,5-Trimethyl aniline	135	N	2.35	
11.50	2,3,5-Trimethyl aniline	135	N	1.21	
23.37	Mannich base (24DMP-mt)	241	N		2.78
23.42	Bis(2-hydroxy, 3,5-dimethylbenzene) methane	256	N	0.46	8.23
24.21	Mannich base (24DMP-35x)	255	N	0.90	
Residual				5.78	6.27
Total				100.00	100.00

^a Assignments confirmed by: L = literature, M = model compound, N = NIST MS library.

phenolic dimer was observed with a methylene proton resonance at 3.85 ppm.



Therefore, the resonance at 3.86 ppm can be assigned to the formation of a bisphenolic methylene structure. Such a reaction has been reported before in other Mannich base systems [13,14,27–35]. Kimura et al. showed that significant methylene species were formed during the polymerization of a monofunctional polybenzoxazine based upon *p*-cresol and aniline [36].

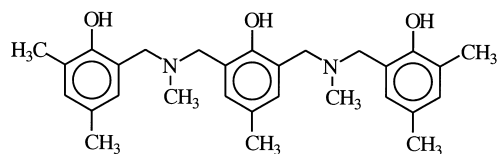


However, when the phenolic group was removed (via reaction with an epoxy during the curing process), the formation of the bisphenolic methylene species did not occur [36]. Russell et al. also proposed the formation of a methylene bridged species during the later stages of cure

above 200°C in the case of difunctional benzoxazines based on Bisphenol-A and aniline [6]. 24DMP-mt also exhibits the resonances at 3.85 ppm, albeit less intense.

Since the *meta* positions on the phenolic portion have not been shown to react at the curing temperatures used in this study [5,6,8,27–35,37], the remaining methylene linkages in this region probably connect the phenolic ring with various locations on the arylamine ring. However, the possible presence of methoxy structures complicates the assignment of these methylene resonances, since the methoxy proton resonance should appear in this vicinity. Also, hydrogen abstraction during ring opening can produce an opening Mannich base with a *N*-methyl group.

The Mannich base methylene carbons of the polybenzoxazine trimer based on 2,4-dimethyl phenol, *p*-cresol, and methylamine (2:1:2) have a resonance at 3.65 ppm [38].



Replacement of an electron-donating benzylic group with an electron-withdrawing aromatic ring (in the case of the *N*-methyl Mannich base) could shift the resonance downfield to the 3.8 ppm region. The smaller resonances between 3.90

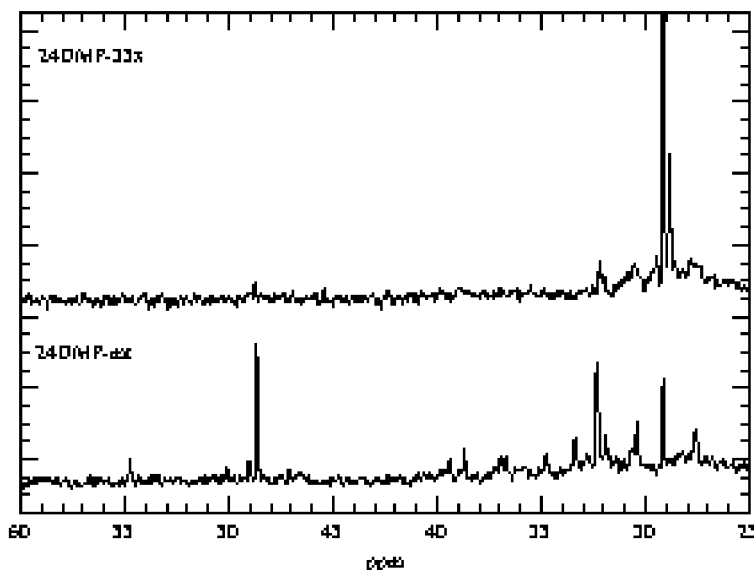


Fig. 5. Methylene region of ^{13}C NMR spectra of reacted 24DMP-mt and 24DMP-35x.

and 4.07 ppm in 24DMP-35x may be due to longer chain oligomeric structures rather than dimeric compounds.

The lower number of arylamine Mannich bridge structures in 24DMP-35x and the corresponding increase in methylene-bridged arylamines, may indicate that the arylamine Mannich bridge structures are simply less thermally stable and, therefore, degrade rapidly enough that few can be observed by NMR. Solomon et al. [28,30,31] indicated that benzylamine structures reacted to the *para* position of 2,6-dimethyl phenol were less stable due to the absence of the intramolecular hydrogen bond between the phenolic hydrogen and the nitrogen. These structures decomposed at lower temperatures to yield methylene bridges at the *para* position. Benzylamine structures linked to the *ortho* position were more stable and remained in the cured resin until much higher temperatures. Therefore, the formation of *para*-linked methylene bridges dominated at lower temperatures while *ortho*-linked methylene bridges dominated at higher temperatures. Sprung et al. showed that the reactivity of 3,5-dimethyl phenol was approximately 7.75 times greater than phenol [39]. A similar situation might be expected to occur with 3,5-dimethyl aniline relative to aniline. Therefore, reaction to the activated *para* position on the arylamine ring is expected to increase as the number of activating methyl groups on the *meta* positions increases. Degradation of these Mannich bridges would produce methylene bridges at the *para* arylamine ring position. In addition, the larger number of polymerization/degradation events will also increase the number of *ortho-ortho* phenolic methylene bridges. Support for these assignments can be found in the evolved gas analysis of the volatiles released from the thermally degraded compounds as shown in Table 2. In this case, 17% by weight *p*-cresol was added as an initiator to accelerate the curing reaction so that enough molecular species were formed to ensure that adequate

mass spectra could be obtained. The *ortho-ortho* phenolic dimer is observed at a retention time near 23.4 min.

3.3. ^{13}C NMR spectroscopy

The methylene region of the ^{13}C NMR spectra of reacted 24DMP-mt and 24DMP-35x is shown in Fig. 5. The resonance at 50.2 ppm (which correspond to one of the methylene carbons in the oxazine ring) is almost completely absent indicating near complete loss of the oxazine ring structure. The intense resonance at 48.6 ppm in 24DMP-mt is assigned to the open ring Mannich base methylene carbon. A resonance corresponding to the methylene carbon of the aromatic Schiff base species mentioned previously is located at 162.5 ppm (not shown). In the case of 24DMP-mt, a resonance corresponding to the phenolic Mannich bridge carbon appears near 49.0 ppm in agreement with the model dimer based on aniline and 2,4-dimethyl phenol mentioned previously [25]. An accompanying new resonance arises at 54.7 ppm. This resonance can be assigned to the other carbon in the arylamine Mannich bridge which is attached to the *para* position on the arylamine ring, since the chemical shift is within 0.2 ppm of the value predicted by simple ^{13}C chemical shift calculations.

A strong resonance appears near 29.2 ppm in both materials. This resonance can be tentatively assigned to the methylene carbon in the methylene linkage attached to the *para* position of the arylamine ring mentioned previously. At extremely long cure times, 24DMP-pt (in which the *para* position of the arylamine is blocked) can react when initiated with 9.1% by weight *p*-cresol and the resonances between 28 and 30 ppm do not appear, although they are observed in 24DMP-mt and 24DMP-35x when cured with the same amount of *p*-cresol. A second prominent resonance appears near 32.2 ppm. This could be attributed to the

Table 3
Calorimetric properties of 4-*t* butyl phenol based-benzoxazine monomers

	Melting temperature (°C)	Peak exotherm (°C)	Heat of reaction (J/g)
4TBUPH-a	75.7	271.9	255.7
4TBUPH-ot	94.9	272.3	224.1
4TBUPH-mt	64.7	265.6	264.9
4TBUPH-pt	90.5	268.6	228.2
4TBUPH-35x	–	247.0	236.4

methylene bridge carbon linked to the *ortho* position of the arylamine ring. The large number of resonances between 30 and 40 ppm are probably the result of a number of various *N*-methyl aniline species and heterocyclic ring species formed at or above 200°C. The interesting peak near 27.6 ppm in 24DMP-mt is very similar to the shift attributed to the methylene linkage between the *ortho* position of phenol and the *ortho* position of the furan ring in novolac/furfuryl alcohol resins cured with hexamethylenetetramine [35]. Benzofuran species have been shown to be formed during the curing of benzoxazine resins [8,37], although the mechanism for their formation has not been elucidated.

3.4. Summary

The addition of methyl substituents at the free *ortho* and *para* sites of the phenolic ring are sufficient to prevent the polymerization of 24DMP-ot and 24DMP-pt. The stabilities of the oxazine rings in these compounds are such that they do not open even when exposed to 200°C for up to 3 h. The presence of methyl substituents at one or both *meta* positions facilitates ring opening at temperatures near or below 200°C. As the temperature is increased to above 190°C, many oxazine rings open in 24DMP-35x. As the temperature is increased, these open rings can thermally cleave and

may react at *para* positions on the arylamine ring to yield arylamine Mannich bridges, which may degrade due to the absence of stabilization by intramolecular hydrogen bonding with the phenolic group. If this degradation occurs, a significant number of methylene linkages to sites on the arylamine ring would be generated.

In the case of 24DMP-mt, the ring cleavage does not happen until slightly higher temperatures such that reaction to activated sites on the arylamine ring occurs in a significant amount. In addition to forming methylene bridges at higher temperatures, 24DMP-mt produces a large variety of additional molecular species that are not readily observed in the case of 24DMP-35x.

3.5. 4-*t*-Butyl phenol-based monomers

In order to determine if the ring-opening polymerization can occur at activated arylamine sites when there is a free *ortho* site on the phenolic ring available, a series of monomers based on 4-*t*-butyl phenol was synthesized. The *t*-butyl phenol protecting group was selected to simulate the bulkiness of the isopropylidene linkage of Bisphenol-A (upon which many thermosetting benzoxazines synthesized in our laboratory are based).

The calorimetric properties of the 4TBUPH-based

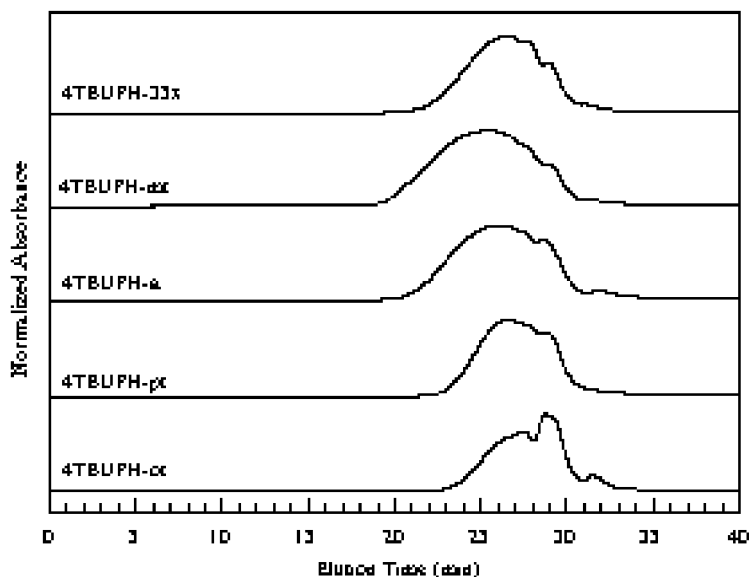


Fig. 6. SEC chromatograms of reacted 4TBUPH-based monomers.

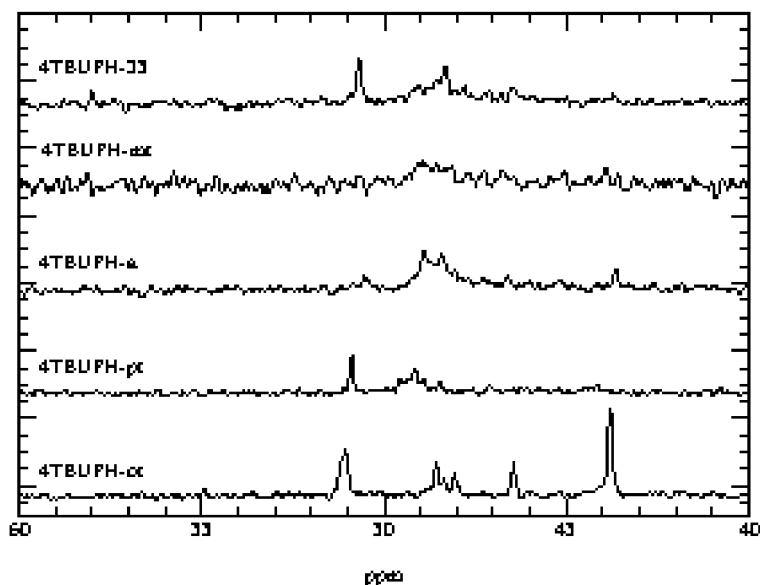


Fig. 7. Methylene region of ^{13}C NMR spectra of reacted 4TBUPH-based monomers.

benzoxazines are listed in Table 3. These materials behave similarly to the 24DMP-based benzoxazines with the addition of a methyl substituent on the *meta* position of the arylamine ring decreasing the peak exotherm temperature and increasing the heat of reaction.

Upon curing, the series of 4TBUPH-based benzoxazines at 190°C for 2 h and 200°C for 1 h (a typical step cure for difunctional benzoxazine resins), SEC was used to examine the molecular weight distribution of the resulting oligomeric species. The SEC chromatograms of the cured materials are shown in Fig. 6. Again, as the *para* position on the arylamine ring is increasingly activated, the molecular weight of the polymerized species increases. It is unknown as to why 4TBUPH-35x does not obey the same pattern as the 24DMP-based series.

3.6. ^{13}C NMR spectroscopy

The methylene region of the ^{13}C NMR spectra of the reacted 4TBUPH-based benzoxazines is shown in Fig. 7. The resonances near 51 ppm indicate that significant amounts of monomer remain for 4TBUPH-ot while almost none remains for 4TBUPH-mt. The open Mannich base again can be found near 48.5 ppm. Unfortunately, it is difficult to accurately determine the Mannich bridge methylene carbon resonances.

While the *t*-butyl tertiary carbon does not differ significantly amongst the materials, the resonances for the methyl carbons differ significantly. An unidentified resonance at about 31.35 ppm appears. As the degree of polymerization increases, i.e. going from 4TBUPH-ot to 4TBUPH-35x, the relative height of this peak steadily diminishes. Around 30.8 ppm, a small resonance appears in 4TBUPH-35x due to the formation of *ortho-ortho* bisphenolic methylene linkages. However, no peaks near 29.2 ppm were observed

indicating that the side reaction, which occurred in the 24DMP-based materials with a blocked *ortho* position is either suppressed totally or does not yield enough material to be observed.

3.7. Summary

The presence of methyl substituents that activate the *para* position on the arylamine ring increases the extent of ring-opening during cure and produces higher molecular weight species. The rings of the non-activated materials are much less likely to fragment and release the free amine at the cure temperatures employed in this study. The extremely large number of fragmented species and end group effects prevent the accurate determination of the regioselectivity from being determined. The secondary crosslinking mechanism of bisphenolic methylene linkage formation occurs in 4TBUPH-35x just as in the previous 2,4-dimethyl phenol-based material. This reaction can dominate the reaction mixture at longer cure times due to its higher thermal stability and obscure the polymerization regioselectivity.

4. Conclusions

The regioselectivity of the ring-opening polymerization of a series of monofunctional benzoxazines based upon methyl-substituted anilines has been examined. Methyl substituents on the *ortho* position of the arylamine ring serve to reduce the basicity of the monomer significantly and sterically hinder the polymerization process. This results in a large number of rings fragmenting upon curing which releases free amine. Methyl substituents in the *meta* position on the arylamine ring facilitate ring-opening/cleavage at lower temperatures. This leads to the secondary reaction, which generates bisphenolic methylene linkages.

Reaction of the oxazine ring to activated sites on the arylamine ring to generate arylamine Mannich linkages can occur at temperatures experienced during reasonable cure regimes. In addition, arylamine Mannich bridges reacted to *para* positions on the arylamine ring may be less thermally stable and may cleave during curing to yield methylene linkages to positions on the arylamine ring.

Acknowledgements

This material is based upon work supported under a National Science Foundation Graduate Fellowship. The authors gratefully acknowledge the partial financial support of the NSF Center for Molecular and Microstructure of Composites (CMMC) which is jointly sponsored by the State of Ohio and the Edison Polymer Innovation Corporation (EPIC), representing industrial members.

References

- [1] Dunkers J, Ishida H. *Spectrochim Acta* 1995;51A:5–855.
- [2] Burke WJ, Glennie EL, Weatherbee C. *J Org Chem* 1964;29:909.
- [3] Burke WJ, Bishop JL, Glennie EL, Bauer Jr. WN. *J Org Chem* 1965;30:3423.
- [4] Reiss G, Schwob JM, Guth G, Roche M, Lande B. In: Culbertson BM, McGrath JE, editors. *Advances in polymer synthesis*. New York: Plenum Press, 1985. p. 27–49.
- [5] Russell VM, Koenig JL, Low HY, Ishida H. *J Appl Polym Sci* 1998;70:1401.
- [6] Russell VM, Koenig JL, Low HY, Ishida H. *J Appl Polym Sci* 1998;70:1413.
- [7] Cid J. PhD Thesis. Case Western Reserve University, 1996.
- [8] Low HY, Ishida H. *Polymer* 1999;40:4365.
- [9] Brunovska Z, Liu JP, Ishida H. *J Macromol Chem Phys* 1999;200:1745.
- [10] Reynolds DD, Cossar BC. *J Heterocycl Chem* 1971;8:597.
- [11] Reynolds DD, Cossar BC. *J Heterocycl Chem* 1971;8:605.
- [12] Reynolds DD, Cossar BC. *J Heterocycl Chem* 1971;8:611.
- [13] Tramontini M. *Synthesis* 1973:703.
- [14] Tramontini M, Angiolini L, Ghedini N. *Polymer* 1988;29:771.
- [15] Miocque M, Vierfond J-M. *Bull Soc Chim Fr* 1970;5:1896.
- [16] Miocque M, Vierfond J-M. *Bull Soc Chim Fr* 1970;5:1901.
- [17] Miocque M, Vierfond J-M. *Bull Soc Chim Fr* 1970;5:1910.
- [18] Tsuchida E, Tomono T. *J Polym Sci A: Polym Chem* 1973;11:723.
- [19] Tsuchida E, Hasegawa E, Tomono T. *J Polym Sci A: Polym Chem* 1974;12:953.
- [20] Tsuchida E, Hasegawa E, Tomono T. *J Polym Sci: Polym Lett* 1974;12:139.
- [21] Tsuchida E, Hasegawa E. *J Polym Sci A: Polym Lett* 1976;12:103.
- [22] Ning X, Ishida H. *J Polym Sci A: Polym Chem*. 1994;32:1121.
- [23] Liu J. PhD Thesis. Case Western Reserve University, 1995.
- [24] Moloney GP, Craik DJ, Iskander MN. *J Pharm Sci* 1992;7:692.
- [25] Kim HD. Unpublished results. Case Western Reserve University.
- [26] Pouchert CJ. *The Aldrich library of NMR spectra*. 2nd ed., vol. 1. Milwaukee, WI: Aldrich Chemical Co, 1983.
- [27] Looney MG, Solomon DH. *Aust. J. Chem* 1995;48:323.
- [28] Zhang X, Looney MG, Solomon DH, Whittaker AK. *Polymer* 1997;38:5835.
- [29] de Bruyn PJ, Foo LM, Lim ASC, Looney MG, Solomon DH. *Tetrahedron* 1997;53:13915.
- [30] Zhang X, Potter AC, Solomon DH. *Polymer* 1998;39:399.
- [31] Zhang X, Solomon DH. *Polymer* 1998;39:405.
- [32] Zhang X, Potter AC, Solomon DH. *Polymer* 1998;39:1957.
- [33] Zhang X, Potter AC, Solomon DH. *Polymer* 1998;39:1967.
- [34] Zhang X, Solomon DH. *Polymer* 1998;39:6153.
- [35] Zhang X, Solomon DH. *Chem Mater* 1998;10:1833.
- [36] Kimura H, Matsumoto A, Hasegawa K, Ohtsuka K, Fukuda A. *J Appl Polym Sci* 1998;68:1903.
- [37] Low HY, Ishida H. *J Polym Sci B: Polym Phys*. 1998;36:1935.
- [38] Krus CM, Ishida H. *Macromolecules* 1998;31:2409.
- [39] Sprung MM. *J Am Chem Soc* 1941;63:335.